Cretaceous Research 29 (2008) 965–975

Contents lists available at ScienceDirect

Cretaceous Research

journal homepage: www.elsevier.com/locate/CretRes

Calcareous nannoplankton, planktonic foraminiferal, and carbonate carbon isotope stratigraphy of the Cenomanian–Turonian boundary section in the Ultrahelvetic Zone (Eastern Alps, Upper Austria)

Michael Wagreich [a,*], Ana-Voica Bojar [b], Reinhard F. Sachsenhofer [c], Stephanie Neuhuber [a], Hans Egger [d]

[a] Department of Geodynamics and Sedimentology, Center for Earth Sciences, University of Vienna, A-1090 Vienna, Austria
[b] Institute of Earth Sciences, Karl-Franzens University, A-8010 Graz, Austria
[c] Department Angewandte Geowissenschaften und Geophysik, MU Leoben, A-8700 Leoben, Austria
[d] Geological Survey of Austria, Neulinggasse 28, A-1030 Vienna, Austria

ARTICLE INFO

Article history:
Received 14 February 2006
Accepted in revised form 4 May 2008
Available online 14 June 2008

Keywords:
Cenomanian-Turonian boundary
Northwestern Tethys
Carbon isotopes
Oxygen isotopes
Nannofossils
Organic geochemistry

ABSTRACT

Ultrahelvetic units of the Eastern Alps were deposited on the distal European continental margin of the (Alpine) Tethys. The Rehkogelgraben section (“Buntmergelserie”, Ultrahelvetic unit, Upper Austria) comprises a 5 m thick succession of upper Cenomanian marl-limestone cycles overlain by a black shale interval composed of three black shale layers and carbonate-free claystones, followed by lower Turonian white to light grey marly limestones with thin marl layers. The main biostratigraphic events in the section are the last occurrence of *Rotalipora* and the first occurrences of *Helvetoglobotruncana helvetica* and *Quadrum gartneri*. The thickest black shale horizon has a TOC content of about 5%, with predominantly marine organic matter of kerogen type II. Vitrinite reflectance and Rock-Eval parameter T_{max} (<424 °C) indicate low maturity. HI values range from 261 to 362 mg HC/g TOC. $\delta^{13}C$ values of bulk rock carbonates display the well documented positive shift around the black shale interval, allowing correlation of the Rehkogelgraben section with other sections such as the Global Boundary Stratotype Section and Point (GSSP) succession at Pueblo, USA, and reference sections at Eastbourne, UK, and Gubbio, Italy. Sediment accumulation rates at Rehkogelgraben (average 2.5 mm/ka) are significantly lower than those at Pueblo and Eastbourne.

1. Introduction

The upper Cenomanian and the Cenomanian-Turonian boundary interval (CTBI) are characterized by widespread deposition of marine organic-rich shales which formed during oceanic anoxic event OAE2 (or Bonarelli event, Schlanger et al., 1987). This anoxic event was associated with a significant extinction event and a turnover in the planktonic realm, including planktonic foraminifera, radiolaria and nannoplankton (e.g., Leckie et al., 2002). A correlation of $\delta^{13}C$ isotope peaks based on the GSSP section at Pueblo (Keller et al., 2004; Kennedy et al., 2005; Sageman et al., 2006) and several other reference sections (e.g., Tsikos et al., 2004; Kuhnt et al., 2005) is possible for both the Tethys, the Atlantic, and the Pacific realms, highlighting the global significance of this event.

In Upper Austria, successions of marls, marly limestones and limestones of the Ultrahelvetic Zone are exposed within several tectonic windows in the Rhenodanubian Flysch Zone. These sediments were deposited in a distal slope environment in northwestern Tethys. The Rehkogelgraben section is the first Cenomanian-Turonian boundary section described from this palaeogeographic setting in the Eastern Alps with a black shale interval. Thus the section provides new information on the evolution of this part of the Tethys during the environmental change from anoxic to oxic sedimentation in the Late Cretaceous (e.g. Hu et al., 2005). Further, it stresses the global significance and widespread distribution of anoxic sediments during the CTBI.

The present paper investigates the biostratigraphy, stable isotope stratigraphy, and sedimentology of the Ultrahelvetic Rehkogelgraben section. Implications for the palaeogeography and the evolution from anoxic to oxic sedimentation in this part of the Tethys are discussed.

2. Geological setting

The Ultrahelvetic units of Austria are remnants of the European continental slope, lying between the Helvetic shelf in the north and

* Corresponding author.
E-mail address: michael.wagreich@univie.ac.at (M. Wagreich).

0195-6671/$ – see front matter © 2008 Elsevier Ltd. All rights reserved.
doi:10.1016/j.cretres.2008.05.017

the abyssal Rhenodanubian/Penninic Flysch basins, a part of the Alpine Tethys of Stampfli et al. (2002), in the south (Faupl and Wagreich, 2000). The shallow-water successions of the Helvetic shelf are characterized by glauconitic sandstones around the Cenomanian-Turonian boundary (e.g., Föllmi, 1989; Hilbrecht et al., 1996) and by the absence of black shales. Further downslope, carbonate-rich cyclic deposits of the Ultrahelvetic units grade into carbonate-depleted marlstones and shales. In the most distal parts of the slope, pure shales, as well as turbidites of the Rhenodanubian Flysch Zone, were deposited below the CCD; in this area, the Cenomanian-Turonian boundary interval is characterized by thick-bedded deep-water sandstones within which no distinct black shale interval has been reported (Mattern, 2002).

The Rehkogelgraben section, described in detail by Kollmann and Summesberger (1982), belongs to an Ultrahelvetic slice between Hagenmühle and Greisenbach, to the east of Gmunden (Upper Austria, Fig. 1a, b). The investigated Cenomanian-Turonian boundary section (coordinates WGS 84: 013° 55′ 30″ E, 47° 56′ 08″ N) includes distinctive black shale horizons and a transition from black shales into marly limestones and red marls, which are typical for Ultrahelvetic sections in Upper Austria (Wendler et al., 2005). These sections are parts of tectonic slices of Ultrahelvetic rocks within the Rhenodanubian Flysch Zone (Fig. 1b). Strata within these tectonic windows have been traditionally attributed to the "Buntmergelserie", an informal lithostratigraphic unit (Prey, 1952) comprising Aptian/Albian to Eocene pelagic and hemipelagic

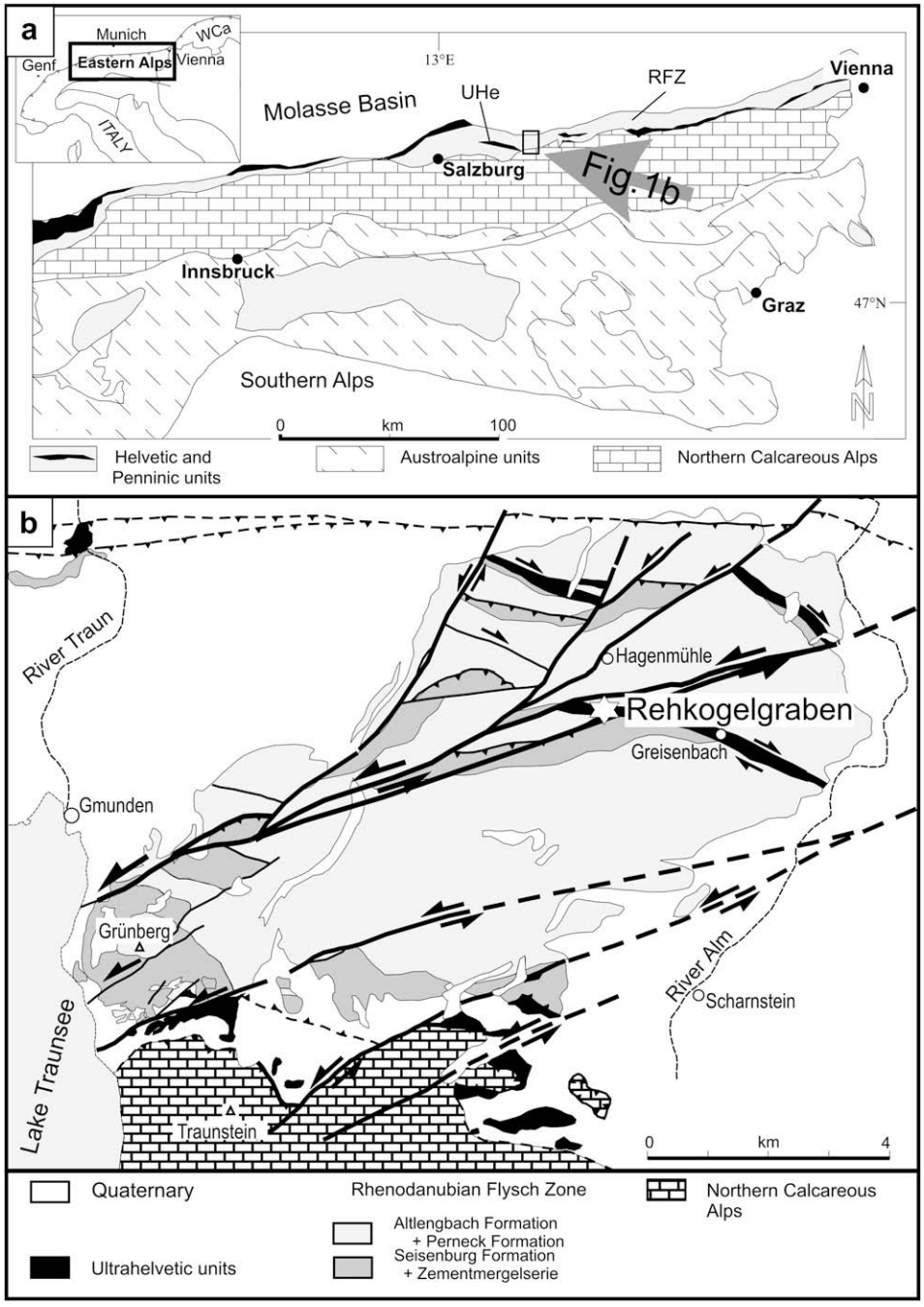

Fig. 1. (a) Tectonic map of the Eastern Alps including slices of Ultrahelvetic units (UHe) within the Rhenodanubian Flysch Zone (RFZ). (b) Geological map of the Rhenodanubian Flysch Zone and the Ultrahelvetic units between Lake Traunsee and Almtal modified from Egger et al. (2000).

shales, marlstones, and marly limestones with rhythmic limestone and marl alterations. Upper to middle bathyal water depths have been inferred for the Ultrahelvetic units (Butt, 1981).

3. Material and methods

The biostratigraphy of the Rehkogelgraben section was investigated using calcareous nannofossils and planktonic foraminifera. For nannofossil investigations, smear slides of 15 samples from the Rehkogelgraben section were prepared using a small piece of sediment and a drop of distilled water. The sediment was smeared onto a glass slide and fixed with canada balsam and then examined under the light microscope.

For the foraminifera investigation, 18 marl, marlstone and claystone samples were disintegrated with hydrogen peroxide and washed over 63–150–300–600 μm sieves. The 150 μm and 300 μm size fractions were richest in planktonic foraminifera for biostratigraphic investigation. Foraminiferal assemblages were checked qualitatively. Additionally, 40 thin-sections of indurated limestone beds were investigated for microfacies and foraminiferal content. However, not all could be used for biostratigraphic zonations because of bad preservation, a low foraminifera numbers, or a lack of carbonate.

Bulk carbon and oxygen isotope contents in carbonates were measured at the Department of Earth Sciences, University of Graz. Powdered bulk rock-samples were analysed due to the presence of strongly indurated limestones, using an automatic Kiel preparation line and a Finnigan MAT Delta Plus mass spectrometer. The standard deviations of the mean values are 0.1% for $\delta^{18}O$ and 0.06% for $\delta^{13}C$. CO_2 was extracted from calcite at 70 °C using a Finnigan MAT Kiel II preparation line. Data were corrected for fractionation using the carbonate–phosphoric acid fractionation factor (Swart et al., 1991). The results of stable-isotope analyses are reported in per mil, relative to the Pee Dee Belemnite Standard (PDB) for carbon and oxygen. For this study, only the isotopic composition of carbonate samples has been measured; as the major black shale interval is carbonate-free, no carbon isotope data from this interval are available.

Powdered samples were analyzed for total carbon content using a Leco C-200 analyser. The total organic carbon content (TOC) was measured on samples pre-treated with concentrated hydrochloric acid.

Black shale samples with TOC contents above 1% were selected for Rock-Eval pyrolysis, carried out using a Rock-Eval 2+ instrument. With this method, the amount of hydrocarbons (mgHC/grock) released from kerogen during gradual heating in a helium stream is normalised against TOC, to give the Hydrogen Index (HI; Espitalié et al., 1977). As a maturation indicator, the temperature of maximum hydrocarbon generation (T_{max}) was measured. Qualitative maceral evaluation was performed on whole rock-samples orientated perpendicular to bedding. Vitrinite reflectance was determined following established procedures (e.g., Taylor et al., 1998) using a Leitz MPV-SP microscope.

4. Results

4.1. Stratigraphy and sedimentology

Athough several faults divide the section into discrete, lithologically uniform blocks, the stream outcrops in the Rehkogelgraben form a composite "Buntmergelserie" section which has been correlated with other sections in the area (e.g. Kollmann and Summesberger, 1982; Prey, 1983). Based on planktonic foraminifera and nannofossils, the composite section includes Albian-Cenomanian dark grey marls and dark to light grey limestones, upper Cenomanian medium grey marls and white limestones, lower Turonian white to light grey limestones, Middle Turonian to Santonian reddish marl-limestone cycles, and lower Campanian red marlstones (Fig. 2).

The CTBI section starts above a fault which separates downstream upper Cenomanian limestones from red to grey marlstones of Turonian-Coniacian age (upstream; Fig. 3). A fairly homogeneous unit (dipping 178/78), with only one minor fault, follows

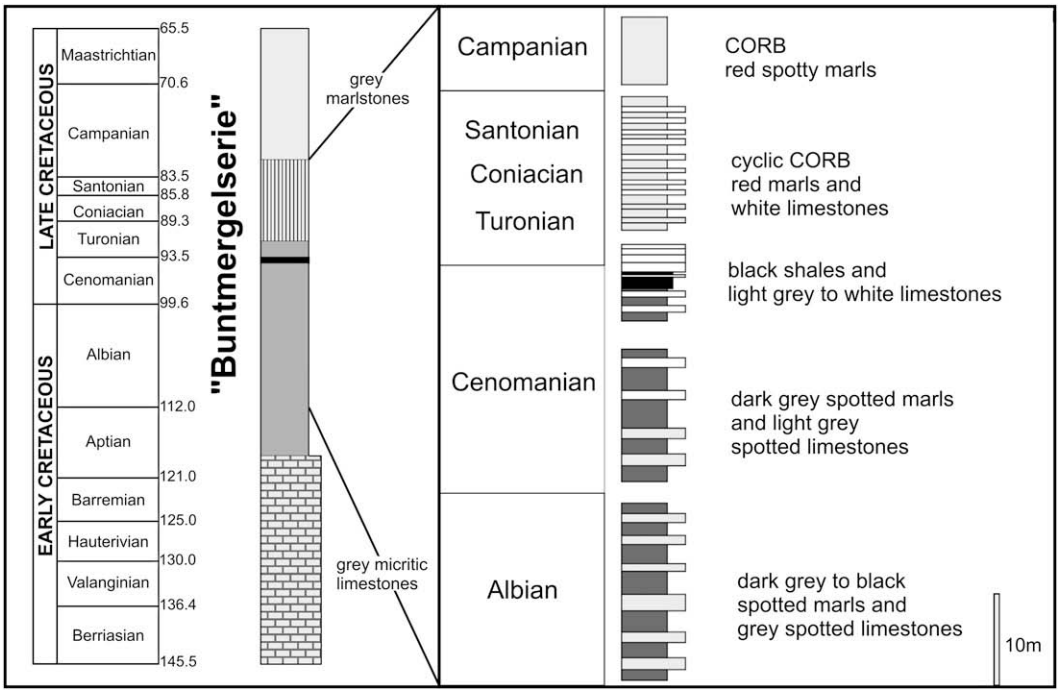

Fig. 2. Schematic log of the Cretaceous of the Ultrahelvetic units in Upper Austria and composite section of the Rehkogelgraben-Greisenbach area according to Rögl in Kollmann and Summesberger (1982), Egger et al. (2000) and new data. CORB – Cretaceous Oceanic Red Beds; timescale from Ogg et al. (2004).

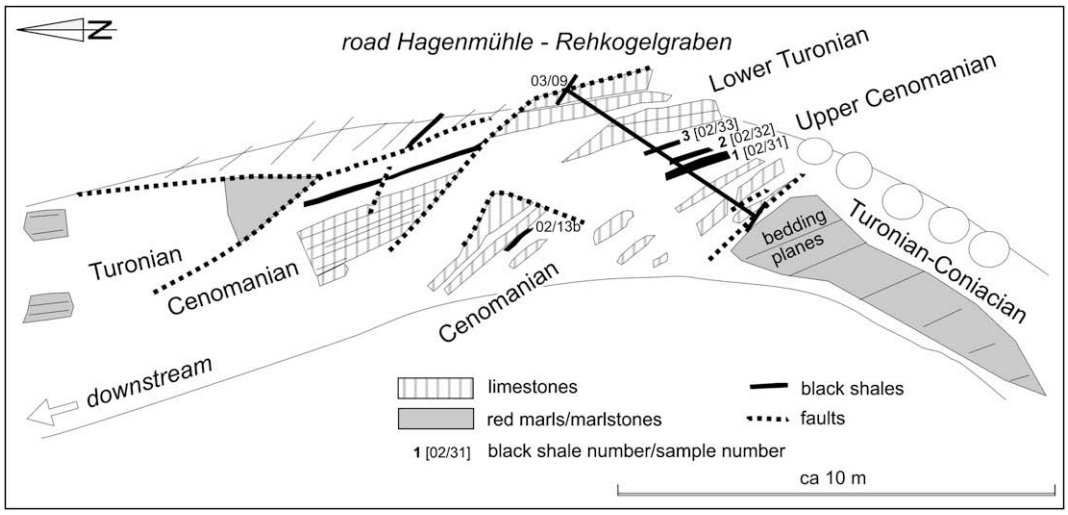

Fig. 3. Sketch of the stream outcrop within the Rehkogelgraben, including the investigated Cenomanian-Turonian boundary section. Faint parallel lines indicate bedding.

downstream terminated by a fault separating the lower Turonian part of the section from two fault blocks of mainly upper Cenomanian strata.

The studied Cenomanian-Turonian boundary section comprises exclusively pelagic and hemipelagic sediments, with no clastic layers such as turbidites, pyroclastic beds, or recognizable bentonite layers. The section (Figs. 4 and 5) starts with a 2.5 m cyclic alternation of light grey, bioturbated pelagic limestones and medium to dark grey pelagic/hemipelagic marls. The carbonate content of limestones varies between 68% and 94%, whereas the interbedded marlstones range between 56% and 73%. About 8 distinct limestones beds are preserved in this part of the section, with some are separated by thick marlstones whilst others are without any marly interbeds (Fig. 5). Microfacies analysis based on thin-sections indicates a predominance of planktonic foraminifera (36–83% of total microfossil assemblages) and calcispheres and very rare benthonic foraminifera (<1%).

Above the last limestone bed, two black shale layers are present (labelled 1 and 2 on Figs. 3 and 5) together with greenish, carbonate-free claystones. This is covered by a thin light grey limestone bed and a third thin black shale-claystone-marl interval (labelled 3 on Fig. 5). Within this 80 cm thick black shale succession, the thickest black shale horizon (1) is 16 cm. Black shales and interbedded claystones are largely devoid of carbonate, with a maximum of 2%. The claystones lack foraminifera but are rich in radiolaria and are interpreted as hemipelagites. TOC values are around 5% in the black shale layers. Limestones between black shale layers 2 and 3 display high abundances of calcispheres (82–93%) and some radiolaria, without significant amounts of planktonic foraminifera.

The overlying upper part of the section is characterized by a 2 m thick succession of white to light grey marly pelagic limestones with no or very thin light grey marl intercalations (<3 cm). The marly limestones to limestones mainly contain calcispheres in the lower part of this interval (up to 88%) with increasing amounts of planktonic foraminifera upsection. Their carbonate contents vary between 65 and 78%. No terrigenous material, other than clay and traces of quartz silt, is present in these pelagic limestones.

Fig. 4. Photograph of Rehkogelgraben outcrop with measured section indicated.

4.2. Biostratigraphy

The biostratigraphic framework of the section is mainly based on calcareous nannofossils with additional information from planktonic foraminifera (Fig. 6). The nannofossil zonations of Perch-Nielsen (1985) and Burnett (1998) have been applied. A late Cenomanian age for the lower part of the section is indicated by the presence of the nannofossils *Lithraphidites acutus* Verbeek and Manivit in Manivit et al., 1977, *Eprolithus floralis* (Stradner, 1962) Stover, 1966, *Quadrum intermedium* Varol, 1992, and *Corollithion kennedyi* Crux, 1981 (nannofossil standard zones CC 10/UC4). *Rotalipora cushmani* (Morrow) and *Rotalipora deeckei* (Franke) are present among other planktonic foraminifera. The onset of the black shale – claystone interval lies above the last occurrences (LO) of *Rotalipora* and *L. acutus*. Due to the lack of carbonate in this part of the profile (from 2.50 to 2.87 m), no direct biostratigraphic dating can be determined. Above the black shale interval, the first appearance (FA) of *Q. gartneri indicates* the base of nannofossil standard zone CC 11 (lower Turonian). This age constraint suggests that the black shale can be attributed to the upper part of CC10 and UC5-6, respectively. Interestingly, the planktonic foraminifera *Helvetoglobotruncana helvetica* (Bolli) has its first occurrence (FO) below *Q. gartneri*. This feature has generally not been observed in other sections (e.g. Luciani and Cobianchi, 1999) and may indicate that the FA for *Q. gartneri* in this section is too high.

The succession of nannofossil events around the Cenomanian-Turonian boundary interval is still under discussion (Burnett, 1998),

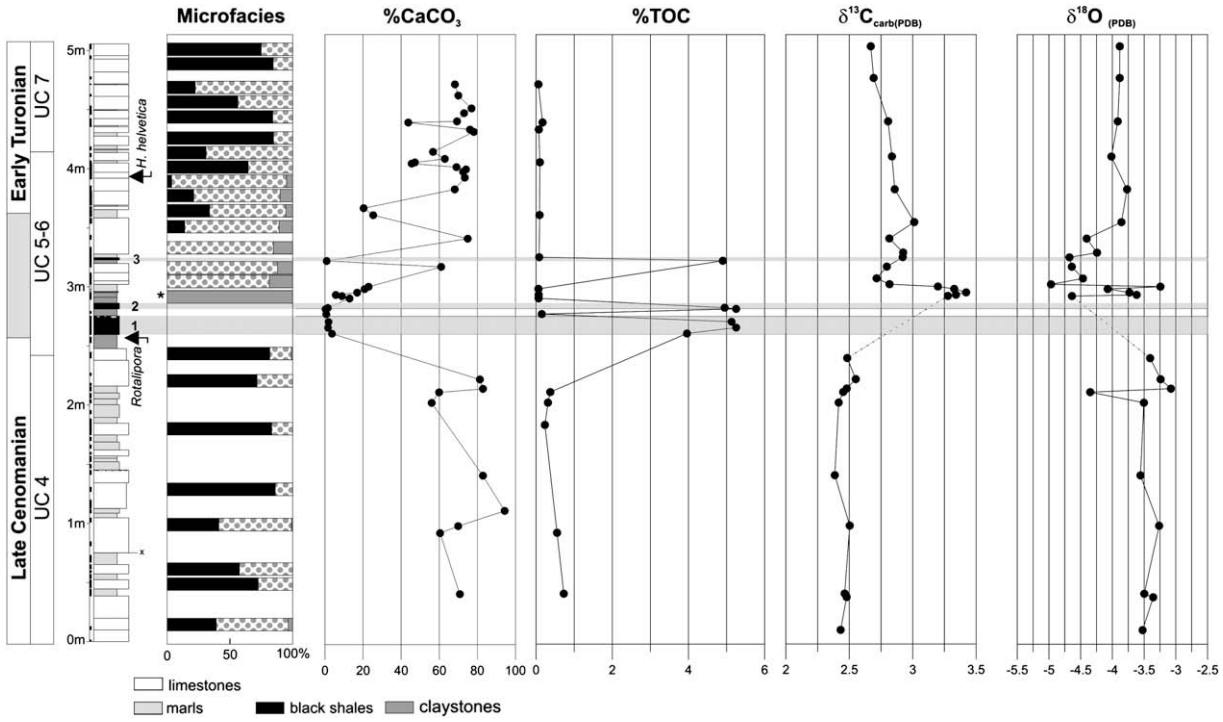

Fig. 5. Sedimentological log of the Rehkogelgraben Cenomanian-Turonian section, including microfacies data based on counts of planktonic foraminifera (black), calcispheres (stippled) and radiolaria (grey) in selected thin sections (except sample marked with * which is a washed residue from a radiolaria-bearing claystone), carbonate and TOC contents, carbon and oxygen isotope values. For detailed biostratigraphy see Fig. 6.

as different sections have given diverse results (e.g. Paul et al., 1994; Luciani and Cobianchi, 1999). Furthermore, the application of a detailed nannofossil biostratigraphy in the Rehkogelgraben section is hampered by the lack of carbonates within the barren black shale interval. The synchronous LO of several species, such as *L. acutus* and *C. kennedyi*, has not been described in other CTBI sections and suggests that a stratigraphic gap exists above the last limestone bed below the black shales, spanning at least the interval from the LO of *C. kennedyi* to the LO of *L. acutus*. *Q. gartneri* is generally regarded as a good marker for the basal Turonian, although some authors, such as Leckie et al. (2002), consider the FO of this marker species to already lie within the upper Cenomanian. Abundance peaks of *E. floralis* are recorded above the black shales and can be correlated with similar peaks at Eastbourne and other CT boundary sections (Paul et al., 1994; Erba, 2004).

4.3. Carbon isotopic composition

The $\delta^{13}C$ isotopic composition displays several excursions in the upper Cenomanian - lower Turonian interval (Fig. 5, Table 1). In the lower part of the section, values lie uniformly around 2.5 ‰ and show a slight decrease before the first small peak of 2.6 ‰, which is associated with the LO of *L. acutus*. The first occurrence of *E. octopetalus* Varol, 1992, above black shale 2, is associated with a second carbon isotope peak of up to 3.4 ‰, followed by a small peak below 3 ‰ immediately after last the increase in TOC, succeed by a final peak of 3 ‰. Towards the top of the section, values progressively decrease down to 2.7 ‰, but never reach values as low as in the upper Cenomanian.

Using the carbon isotope curve, correlations can be made with detailed $\delta^{13}C$ records from the GSSP section at the Pueblo anticline, Colorado, USA (Kennedy et al., 2005) and several other reference sections, such as Gubbio, Italy, and Eastbourne, UK, (Tsikos et al., 2004; Gale et al., 2005; Jarvis et al., 2006), northern Germany (Voigt, 2000), Tunisia (Amédro et al., 2005) and the Crimea (Fisher et al., 2005). Our carbon isotope data are low in resolution, as they were obtained exclusively from calcareous samples and thus display a significant gap within the carbonate-free black shale-claystone interval (Fig. 5). However, several excursions and trends before and after the black shale interval in the $\delta^{13}C$ evolution during the CTBI can be matched and, combined with biostratigraphic marker events, support a correlation with these sections (Fig. 7).

The data indicate that the Rehkogelgraben section clearly starts above the mid-Cenomanian $\delta^{13}C$ event (MCE) which is reported elsewhere from the *Acanthoceras rhotomagense* Zone and the lower part of *Rotalipora cushmani* Zone (e.g., Keller et al., 2004). In the lower part of the Rehkogelgraben section, the first small carbon isotope peak, with values of 2.6 ‰, is biostratigraphically higher than the reported position of the MCE. The first comparable event from the boundary interval at Rehkogelgraben is the onset of the positive $\delta^{13}C$ shift that leads to the characteristic OAE2 peak. This shift starts below the LO of the *Rotalipora* group both at Rehkogelgraben and at Gubbio, whereas at Eastbourne a larger interval is present between these two events (MCE and OAE2). The first $\delta^{13}C$ peak of OAE2, known from Eastbourne and Pueblo (Gale et al., 2005) has not been recognized in the Rehkogelgraben due to the lack of calcareous samples, but is thought to lie within the first major 16 cm black shale horizon 1. The second OAE2 $\delta^{13}C$ peak may thus correspond to the first samples above the carbonate-free interval in the Rehkogelgraben, although the values of up to 3.42 ‰ are lower than those found at Eastbourne but similar to values from the Gubbio section. Above this, a sharp decrease in $\delta^{13}C$ values is followed by the third OAE2 peak, largely similar to the situation at Eastbourne, Gubbio and Sicily (Tsikos et al., 2004; Scopelliti et al., 2004; Jarvis et al., 2006). This peak marks the end of the widely recognized $\delta^{13}C$ plateau (e.g. Gale et al., 2005). All sections, including the Rehkogelgraben, display a gradual decrease of the $\delta^{13}C$ values within the lower Turonian interval. Altogether, the correlation of peaks is good, especially with the pelagic Gubbio section (Fig. 5). Based on the correlation with the GSSP section at Pueblo, where the

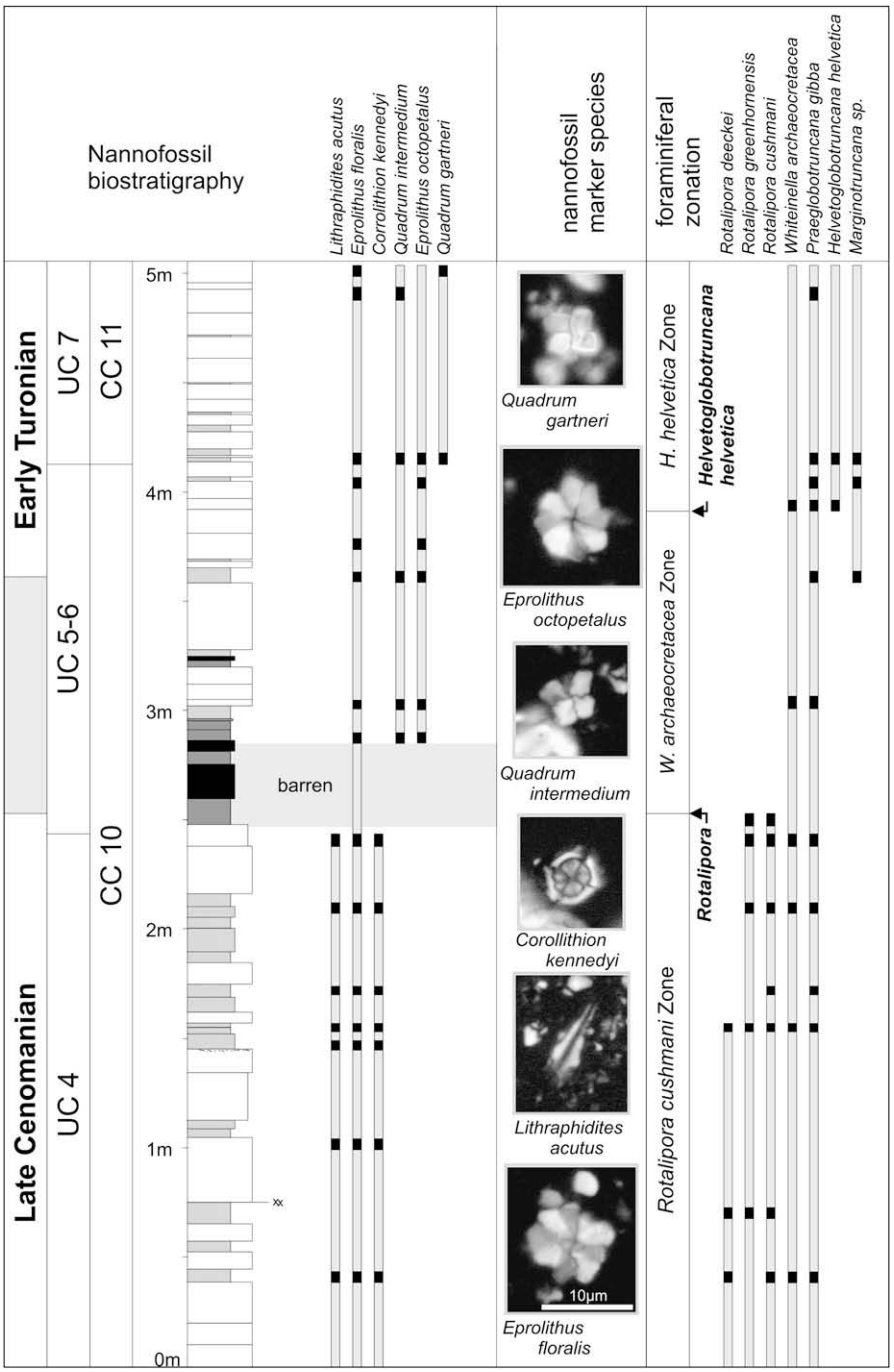

Fig. 6. Nannofossil biostratigraphy and planktonic foraminiferal events in the Rehkogelgraben section. Nannofossil zonations according to Perch-Nielsen (1985) and Burnett (1998); planktonic foraminifera zones according to Caron (1985). Possible interval of Cenomanian-Turonian boundary shaded in grey.

Cenomanian-Turonian boundary has been fixed at the FO of the ammonite *Watinoceras devonense*, the stage boundary should be situated just below the third $\delta^{13}C$ peak, and thus below the FO of *Quadrum gartneri*. In the Rehkogelgraben, this level is clearly above the last black shale horizon 3 (see Fig. 5), which points towards a late Cenomanian age for the major part of OAE2.

4.4. Oxygen isotopic composition

The oxygen isotope values (Fig. 5, Table 1) show an overall decreasing trend over the examined profile, punctuated by smaller second-order oscillations. The values display a significant drop from around −3.5 ‰ PDB before to below −4.5 ‰ after the black shale interval, then rising back to values between −4 ‰ and −3.5 ‰. Based on the $\delta^{13}C/\delta^{18}O$ plot (Fig. 8), the influence of diagenesis is not as evident as expected; a rather low correlation value of $R = 0.1$ between $\delta^{13}C$ and $\delta^{18}O$ indicates no strong diagenetic influence on the isotope values.

4.5. Organic carbon contents, thermal maturity and organic geochemistry

The total organic carbon (TOC) content varies significantly in the studied interval of the Rehkogelgraben profile (Fig. 5). TOC values in the upper Cenomanian marlstones are low and decrease upwards from 0.7 to 0.2%. TOC contents in the black shales vary between 4.0

Table 1
$\delta^{13}C_{carbonate}$ and $\delta^{18}O$ data from the Rehkogelgraben section (Ultrahelvetic unit, Upper Austria)

m above base of section	$\delta^{13}C$ (PDB)	$\delta^{18}O$ (PDB)
5.10	2.67	−3.88
4.83	2.69	−3.88
4.46	2.81	−3.92
4.16	2.84	−4.02
3.88	2.86	−3.77
3.60	3.01	−3.86
3.46	2.82	−4.40
3.34	2.92	−4.24
3.30	2.92	−4.68
3.22	2.80	−4.64
3.12	2.71	−4.46
3.07	2.82	−4.97
3.05	3.20	−3.24
3.03	3.33	−4.07
3.00	3.42	−3.73
2.98	3.34	−3.62
2.97	3.28	−4.64
2.44	2.48	−3.40
2.26	2.55	−3.24
2.18	2.48	−3.08
2.15	2.45	−4.35
2.06	2.42	−3.50
1.44	2.39	−3.56
1.01	2.50	−3.26
0.43	2.46	−3.50
0.40	2.48	−3.36
0.12	2.43	−3.52

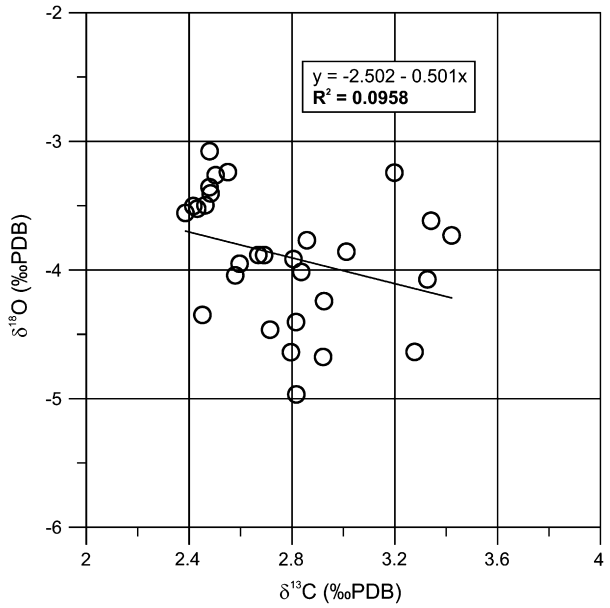

Fig. 8. Cross correlation of $\delta^{13}C$ and $\delta^{18}O$ from samples of the Rehkogelgraben section. No significant co-variance can be detected.

and 5.1%, whereas the claystones and marly claystones located between the black shales have very low TOC contents (0.07–0.15%). TOC contents in the lower Turonian section above the black shale interval remain low (<0.2%) and are lower than the Cenomanian part.

A Cenomanian black shale, with abundant *Rotalipora*, e.g. *Rotalipora cushmani*, occurs in an isolated, fault-bound block close to the logged profile (sample 02/13b in Fig. 3). Although it is definitely older than the black shales of the CTBI profile, because of the presence of several species of *Rotalipora*, its exact stratigraphic position and its relation to the CTBI section remains unclear due to faulting. The TOC content of this black shale is only 1.0%.

Vitrinite reflectance (0.45%Rr) and Rock-Eval parameter T_{max} (418–424 °C) indicate a low maturity of organic matter. HI values range from 261 to 362 mg HC/g TOC and increase with stratigraphic age (Fig. 9). The Cenomanian black shale below the logged profile (sample 02/13b) is characterized by the highest recorded HI value

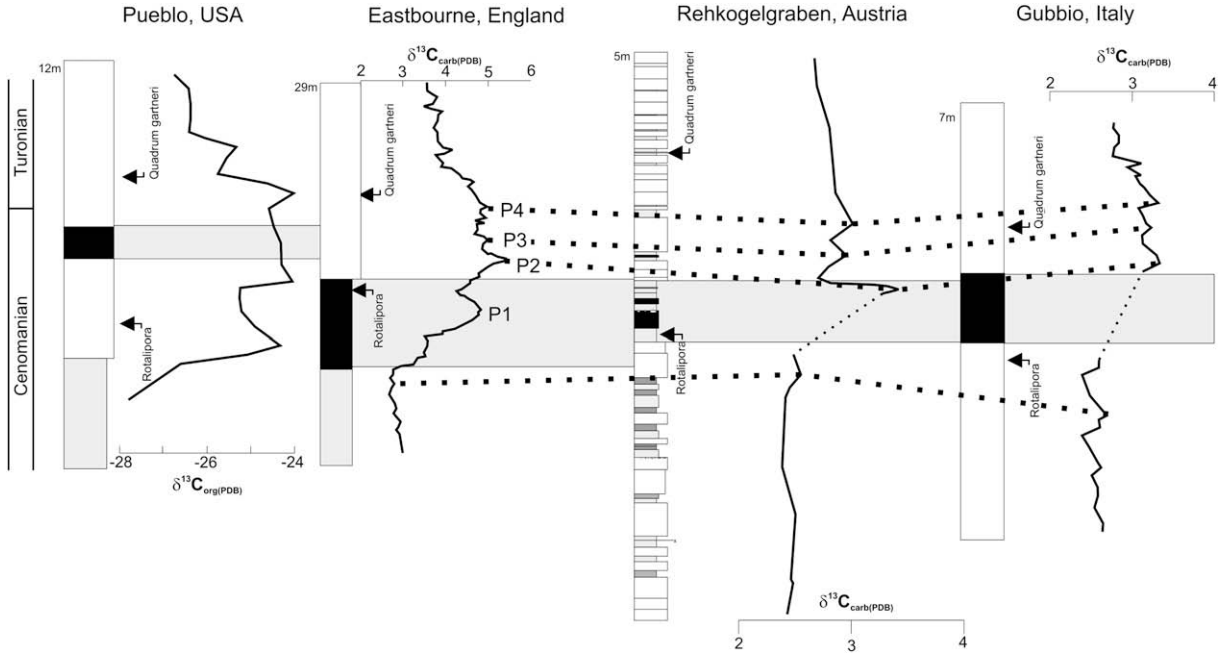

Fig. 7. Chemo- and biostratigraphic correlation between the Cenomanian-Turonian boundary sections of Pueblo (GSSP stratotype; Tsikos et al., 2004), Eastbourne (Paul et al., 1999; Tsikos et al., 2004), Rehkogelgraben and Gubbio (Tsikos et al., 2004). Note different scale of sections. Correlation level taken at onset of $\delta^{13}C$ excursion and at the Cenomanian-Turonian boundary from the Pueblo section. Grey shaded areas are intervals of TOC maximum and carbonate minimum defined by Tsikos et al. (2004). P1 to P4 denote $\delta^{13}C$ peaks identified at Eastbourne and correlated to Rehkogelgraben and Gubbio.

(362 mg HC/g TOC). The mean HI value of two samples from black shale 1 is 332 mg HC/g TOC, whereas the HI of black shale 2 is 296 mg HC/g TOC. The HI value from the uppermost black shale layer is even lower (261 mg HC/g TOC). These values are typical for type II kerogen, which is usually related to marine organic matter (Tissot and Welte, 1984). The decrease towards slightly lower values towards the top of the profile might indicate an increased contribution of terrestrial organic matter, or stronger bacterial degradation. There is no clear relation between the TOC and HI values, although both TOC and HI show a slight decrease from black shale intervals 1 to 3.

Optical microscopy reveals that the organic matter consists mainly of marine material (lamalginite, telalginite) although terrestrially derived material (vitrinite, reworked vitrinite, and inertinite) is also present (Fig. 10). Apart from relatively large alginite bodies, tiny liptodetrinite particles contribute significantly to the organic matter. Inertinite (up to several millimetres long) is probably of aeolian origin. An even larger vitrinite particle (9 mm in length) occurs in black shale 1 and indicates a terrestrial influence.

The TOC contents within the black shales are not as high as reported for the Bonarelli level from classical Italian sections (e.g., 23%, Coccioni and Luciani, 2004; 26.5%, Scopelliti et al., 2004). However, HI values are in a similar range (200–400 mg HC/g TOC; Scopelliti et al., 2004) indicating similar sources for marine organic matter.

5. Discussion

The integration of biostratigraphic, micropaleontological and geochemical data obtained from the Rehkogelgraben section provides significant information on the timing and palaeoceanographic evolution of OAE2 within the northwestern Tethys (Penninic Ocean of Faupl and Wagreich, 2000; Alpine Tethys of Stampfli et al., 2002) at the southern continental slope of the European platform. Cenomanian-Turonian boundary strata from similar palaeographic settings have rarely been described from the Alps, especially from the Austrian and Swiss Alps. Helvetic units include mainly shallow water neritic successions and even in the most pelagic units in western Austria, the Cenomanian-Turonian boundary interval is characterized by the occurrence of glauconitic sandstones (Götzis Beds) within the pelagic Seewen limestone (Föllmi, 1989). Similar glauconitic sands and hemipelagic marls (Plenus Marls) are also known from the Regensburg embayment (southern Germany) and the autochthonous Cretaceous in the basement of the Cenozoic Molasse basin (Hilbrecht et al., 1996). Pelagic Ultrahelvetic successions include minor dark grey and black shales and are only known from the Ultrahelvetic Liebenstein Nappe of Vorarlberg (western Austria), where the Cenomanian-Turonian boundary interval already lies within the pelagic Liebenstein limestone and no distinct OAE2 black shales horizons have been documented so far from this unit (Weidich, 1987).

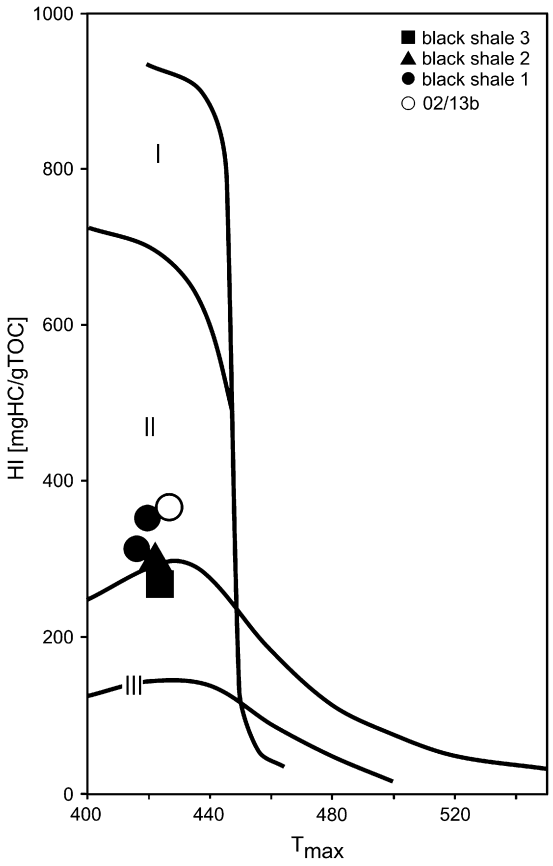

Fig. 9. Rock-Eval diagram of hydrogen index versus Tmax; kerogen types according to Tissot and Welte (1984). Black shale numbers 1–3 refer to the Cenomanian-Turonian boundary interval (Fig. 5); sample number 02/13b refers to the Cenomanian black shale (Fig. 3).

The palaeogeographic position of the studied section, at the distal part of the European continental margin of the Ultrahelvetic units in Upper Austria, resembles distant successions such as the Vocontian trough in France. Further, similarities are present in successions of the Subbrianconnais units of Switzerland, such as at the Prealpes Romandes, were mid-Cretaceous black shales are overlain by red pelagic formations (“couches rouges”, Strasser et al., 2001) and the Pieniny Klippen Belt and the Silesian/Subsilesian units of the Western Carpathians, which also comprise deep-water pelagic deposits south of the European platform (Bak et al., 2005; Bak, 2006). With respect to the low carbonate contents of black shales and TOC peak contents of around 5%, the section displays similarities to the Bonarelli Level in the Dolomites (Luciani and Cobianchi, 1999), which may have been situated at the southern margin of the Alpine Tethys during this time.

The $\delta^{13}C$ data from the Rehkogelgraben enable a correlation to be made with other Cenomanian-Turonian boundary sections, including the GSSP section at Pueblo and the reference sections of Gubbio and Eastbourne. This correlation, based on biostratigraphic events and carbon isotopes, allows the estimation of sedimentation rates based on various age models for the CTBI. Total durations of OAE2, based on Milankovitch cyclicity (mainly precession cycles), have been estimated to range between 240 ka (Paul et al., 1994: 12 cycles), 360 ka (Prokoph et al., 2001: 22.5 cycles), 440 ka (Kuhnt et al., 2005: 11 cycles), about 700 ka (Keller and Pardo, 2004), and 563–601 ka (Sageman et al., 2006). Estimations on average sedimentation rates (without decompaction) at Pueblo give 27 mm/ka at the onset of OAE2 in the late Cenomanian and 7.5 to 9.5 mm/ka for the major part (600 ka) of the $\delta^{13}C$ plateau (Snow et al., 2005). These sedimentation rates are based on several biostratigraphic events, such as the LO of the genus *Rotalipora,* reported at 93.90 Ma, and the FO of *Helvetoglobotruncana helvetica* at 93.29 Ma according to Keller and Pardo (2004).

Correlation to the Rehkogelgraben section using the chronostratigraphic framework of Keller and Pardo (2004) and Snow et al. (2005) indicates an average sedimentation rate of 2.5 mm/ka for the Rehkogelgraben. This value, which is very similar to an average sedimentation rate of about 2.3 mm/ka calculated using a different time-scale, based on graphic correlation of the section (Bob Scott, pers. comm., 2005), lies significantly below that given in most other sections, such as 10 mm/ka in Gubbio (Coccioni and Luciani, 2004), 30 mm/ka at Eastbourne (Prokoph et al., 2001), 170 mm/ka in the Tarfaya Basin (Kuhnt et al., 2005). Thus, sedimentation rates in the Rehkogelgraben are relatively low compared to most other sections as a consequence of the pelagic depositional

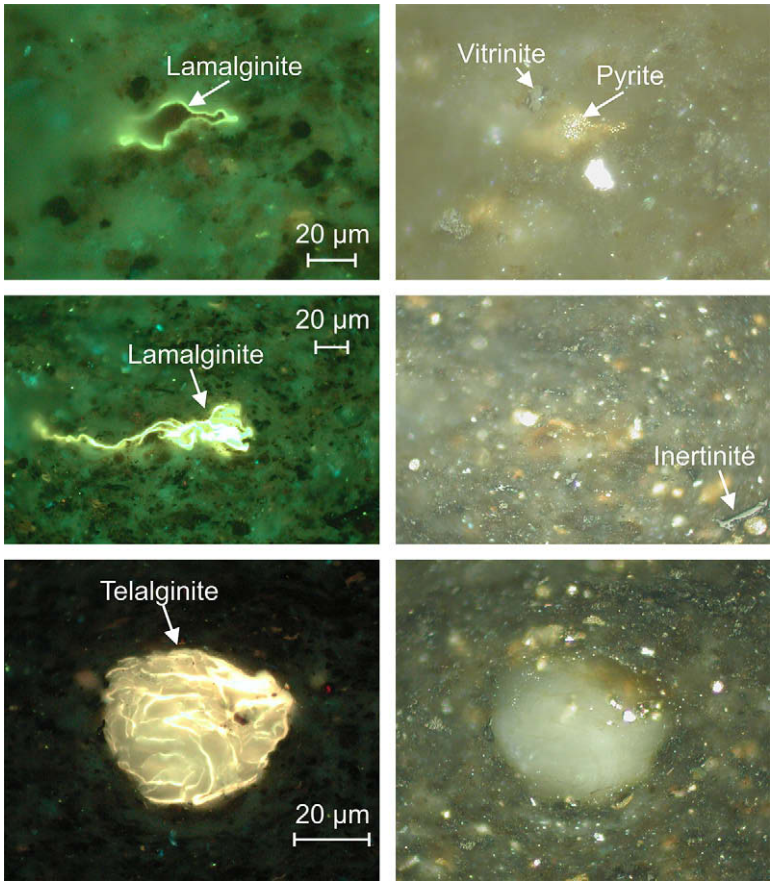

Fig. 10. Photomicrographs of black shale 1 (oil immersion, sample REH02/31). Each photo was taken using blue light irradiation (left column) and incident white light (right column). Lamalginite is present in significant amounts together with minor vitrinite and inertinite (upper pictures). Telalginite (lower pictures) is observed rarely.

setting, far from any terrigenous input. Nevertheless, the coeval last appearance of several nannofossil markers in the upper Cenomanian also suggests a possible hiatus on top of the last limestone bed below black shale 1.

The $\delta^{18}O$ fluctuation around the Cenomanian- Turonian boundary may be due to diagenesis, since oxygen isotopes in carbonates are more affected by diagenesis compared to carbon isotopes. However, part of the fluctuation could be attributed to the difference in $\delta^{18}O$ in ocean water as a result of temperature change and/or influx of freshwater. The observed pattern in oxygen correlates broadly with that found at Eastbourne and Gubbio (comp. Tsikos et al., 2004). However, because the sample resolution is considerably lower in the Rehkogelgraben profile, no detailed correlations can be made. The most prominent feature includes less variable values until the first carbon peak associated with a negative excursion for oxygen and subsequent recovery to values up to -3 ‰. At both Rehkogelgraben and Eastbourne, this carbon peak is associated with a positive excursion for oxygen, subsequent decrease and recovery to constant values around -3.7 ‰ during the early Turonian. For all sections, including Eastbourne, Gubbio, and Rehkogelgraben, the values for the late Cenomanian are higher than those for the early Turonian. Further studies, using additional palaeoceanographic proxies, may solve these questions.

Another conspicuous feature of the Rehkogelgraben section is the presence of a carbonate-poor black shale interval. A significant crisis in the deposition of carbonate or a carbonate dissolution event was noted as an additional feature of the CTBI (e.g. Hilbrecht et al., 1996; Voigt, 2000), including a drowning event on carbonate platforms and a change in platform carbonate mineralogy from aragonite- to calcite-dominated assemblages (Steuber, 2002). The Rehkogelgraben section illustrates the presence of such a carbonate crisis, the carbonate content dropping from between 56 and 94% to 0 to 3% within the black shale interval. Black shales are largely carbonate free, and the intercalated TOC-poor sediments around the first and second black shale horizons are greenish-grey claystones devoid of carbonate.

The lack of preserved carbonate concomitant with increased TOC levels indicates a global eutrophication, in which the oxygen minimum zone lies within the water column and prevents oxic degradation of organic matter. This most likely causes a positive feedback as more nutrients, such as PO_4 and NO_3, are released during anoxic organic matter degradation which drives further growth of surface dwelling organisms. Three distinct layers of TOC enrichment can be observed in the Rehkogelgraben profile. The claystone between label 1 and label 2 in Fig. 5 shows low TOC and low $CaCO_3$ contents between two TOC spikes. This might indicate a strong decline in primary production caused by a local shift of the oxygen minimum zone towards the surface of the ocean.

A qualitative evaluation of limestone thin-sections indicates a strong shift in microfossil assemblages from planktonic foraminifera below the first black shale interval to calcispheres (various types of dinoflagellate cycsts) above the first level. Above the second black shale bed, carbonate values display a gradual increase from below 10% to about 61% in the first limestone bed. The following lower Turonian limestones do not reach such high values as the limestones at the base of the section and stay below 77%, indicating a relatively long recovery period for calcareous plankton after the oceanic anoxic event (Harries, 1999).

Intensive submarine volcanism during the formation of the Ontong-Java and Caribbean plateaus, a sea-level rise during an

extremely high long-term sea level and high levels of atmospheric carbon dioxide (e.g., Jones and Jenkyns, 2001; Snow et al., 2005) have been proposed as trigger mechanisms for the OAE2. Short-time volcanic forcing of an already poorly oxygenated ocean over a threshold into anoxic state is suggested as one cause for OAE2 (Snow et al., 2005). The extinction of the deep-dwelling planktonic foraminifera group *Rotalipora* at the onset of OAE2 may have been a result of the combined effect of an expanding oxygen minimum zone, biolimiting or toxic concentrations of metals by hydrothermal plumes, and may have been to some extent due to increased competition from evolving dicarinellids (Leckie et al., 2002; Keller and Pardo, 2004; Snow et al., 2005). No peak in the oxygen minimum zone dwellers of the heterohelicid group (Keller and Pardo, 2004) has been observed within the Rehkogelgraben section, but this may be due to the overall lack of carbonate within the major part of OAE2. In the Rehkogelgraben succession, the low carbonate content below and above black shale level 1, together with the coeval deposition of marls, may indicate higher detrital influxes due to transgression and/or fresh water influx.

The positive $\delta^{13}C$ shift and the marine kerogen-type of the organic matter as recognized also in the Rehkogelgraben section, suggest increased productivity of oceanic surface waters and enhanced preservation and burial as the main palaeoceanographic features associated with OAE2 (e.g. Leckie et al., 2002). The associated faunal turnovers (e.g. Erba, 2004; Keller and Pardo, 2004) indicate major changes in water mass stratification such as a global stagnation of ocean circulation and an abrupt warming of intermediate and deep-waters (Huber et al., 1999; Leckie et al., 2002).

6. Conclusions

The Rehkogelgraben section of the "Buntmergelserie", an Ultrahelvetic unit, comprises the first black-shale bearing Cenomanian-Turonian boundary section from the Eastern Alps so far documented. The succession was deposited on the distal European continental margin of the (Alpine) Tethys. Black shales occur within a carbonate-depleted to carbonate-free interval, which marks the consequences of a significant carbonate crisis during this time, at least in the Tethyan realm. High TOC contents (up to 5%) and predominantly marine organic matter are similar to other OAE2 successions such as the Bonarelli-level in Italy. Nannofossil biostratigraphy, planktonic foraminifera events, and $\delta^{13}C$ chemostratigraphy enable a correlation with several Cenomanian-Turonian boundary sections, notably Gubbio (Italy) and Eastbourne (U.K.). Sedimentation rates at the Rehkogelgraben are significantly lower than most other Cenomanian-Turonian boundary OAE2 sections as a consequence of the pelagic depositional setting of the Ultrahelvetic units, and a possible gap in sedimentation during the upper Cenomanian.

Acknowledgements

This paper is a contribution to IGCP 463 "Upper Cretaceous Oceanic Red Beds" and IGCP 555. Field work was supported by the Austrian Academy of Sciences. For reviewing an earlier version of the manuscript we thank Sebastian Lüning (Bremen). Reviews by H. Tsikos (Grahamstown) and K. Bak (Krakow) greatly improved the manuscript.

References

Amédro, F., Accarie, H., Robaszynski, F., 2005. Position de la limite Cénomanien-Turonien dans la Formation Bahloul de Tunisie centrale: apports intégreés des ammonites et des isotopes du carbone ($\delta^{13}C$). Eclogae Geologicae Helvetiae 98, 151–167.

Bak, K., 2006. Sedimentological, geochemical and microfaunal responses to environmental changes around the Cenomanian–Turonian boundary in the Outer Carpathian Basin; a record from the Subsilesian Nappe, Poland. Palaeogeography Palaeoclimatology Palaeoecology 237, 335–358.

Bak, K., Barski, M., Bak, M., 2005. High resolution microfossil, microfacies and palynofacies studies as the only method in recognition of the Jurassic and Cretaceous "black shales" in a strongly tectonised section of the Czorsztyn Succession, Pieniny Klippen Belt, Poland. Studia Geologica Polonica 124, 171–198.

Burnett, J.A., 1998. Upper Cretaceous. In: Bown, P.R. (Ed.), Calcareous Nannofossil Biostratigraphy. Chapman & Hall, Cambridge, pp. 132–199.

Butt, A., 1981. Depositional environments of the Upper Cretaceous rocks in the northern part of the Eastern Alps. Cushman Foundation for Foraminiferal Research Special Publication 20, 1–81.

Caron, M., 1985. Cretaceous planktonic foraminifera. In: Bolli, H.M., Saunders, J.B., Perch-Nielsen, K. (Eds.), Plankton Stratigraphy. Cambridge University Press, Cambridge, pp. 17–86.

Coccioni, R., Luciani, V., 2004. Planktonic foraminifera and environmental changes across the Bonarelli Event (OAE2, latest Cenomanian) in its type area: a high resolution study from the Tethyan reference Bottaccione section (Gubbio, Central Italy). Journal of Foraminiferal Research 34, 109–129.

Crux, J.A., 1981. New calcareous nannofossil taxa from the Cretaceous of South England. Neues Jahrbuch für Geologie und Paläontologie, Monatshefte 1981, 633–640.

Egger, J., Kollmann, H.A., Sanders, D., Summesberger, H., Wagreich, M., 2000. Cretaceous of eastern Austria. In: Field Trip Guide 6th International Cretaceous Symposium, Vienna, 2000, pp. 1–56.

Erba, E., 2004. Calcareous nannofossils and Mesozoic oceanic anoxic events. Marine Micropaleontology 52, 85–106.

Espitalié, J., LaPorte, J.L., Madec, M., Marquis, F., Leplat, P., Paulet, J., Boutefeu, A., 1977. Méthode rapide de charactérisation des roches mères de leur potential pétrolier et de leur degré dévolution. Revue de Ílnstitut Francais du Pétrole 32, 23–42.

Faupl, P., Wagreich, M., 2000. Late Jurassic to Eocene palaeogeography and geodynamic evolution of the Eastern Alps. Mitteilungen der Österreichischen Geologischen Gesellschaft 92, 79–94.

Fisher, J.K., Price, G.D., Hart, M.B., Leng, M.J., 2005. Stable isotope analysis of the Cenomanian-Turonian (Late Cretaceous) oceanic anoxic event in the Crimea. Cretaceous Research 26, 853–863.

Föllmi, K.B., 1989. Evolution of the mid-Cretaceous triad. Lecture Notes in Earth Sciences 23, 1–153.

Gale, A.S., Kennedy, W.J., Voigt, S., Walaszcyk, I., 2005. Stratigraphy of the Upper Cenomanian-Lower Turonian Chalk succession at Eastbourne, Sussex, UK: ammonites, inoceramid bivalves and stable carbon isotopes. Cretaceous Research 26, 460–487.

Harries, P.J., 1999. Repopulations from Cretaceous mass extinctions: environmental and/or evolutionary controls? In: Barrera, E., Johnson, C.C. (Eds.), Evolution of the Cretaceous Ocean-Climate System. Geological Society of America Special Paper 332, 345–364.

Hilbrecht, H., Frieg, C., Tröger, K.-A., Voigt, S., Voigt, T., 1996. Shallow water facies during the Cenomanian-Turonian anoxic event: Bio-Events, isotopes and sea level in southern Germany. Cretaceous Research 17, 229–253.

Hu, X., Jansa, L., Wang, C., Sarti, M., Bak, K., Wagreich, M., Michalik, J., Soták, J., 2005. Upper Cretaceous oceanic red beds (CORBs) in the Tethys: occurrences, lithofacies, age, and environments. Cretaceous Research 26, 3–20.

Huber, B.T., Leckie, R.M., Norris, R.D., Bralower, T.J., CoBabe, E., 1999. Foraminiferal assemblage and stable isotope change across the Cenomanian-Turonian boundary in the subtropical North Atlantic. Journal of Foraminiferal Research 29, 392–417.

Jarvis, I., Gale, A.S., Jenkyns, H.C., Pearce, M.A., 2006. Secular variation in Late Cretaceous carbon isotopes: a new $\delta^{13}C$ carbonate reference curve for the Cenomanian–Campanian (99.6–70.6 Ma). Geological Magazine 143, 561–608.

Jones, C.E., Jenkyns, H.C., 2001. Seawater strontium isotopes, oceanic anoxic events, and seafloor hydrothermal activity in the Jurassic and Cretaceous. American Journal of Science 301, 112–149.

Keller, G., Berner, Z., Adatte, T., Stueben, D., 2004. Cenomanian–Turonian and δ13C, and $\delta^{18}O$, sea level and salinity variations at Pueblo, Colorado. Palaeogeography Palaeoclimatology Palaeoecology 211, 19–43.

Keller, G., Pardo, A., 2004. Age and paleoenvironment of the Cenomanian-Turonian global stratotype section and point at Pueblo, Colorado. Marine Micropaleontology 51, 95–128.

Kennedy, W.J., Walaszczyk, I., Cobban, W.A., 2005. The global boundary stratotype section and point for the base of the Turonian stage of the Creataceous: Pueblo, colorado. Episodes 28, 93–104.

Kollmann, H.A., Summesberger, H., 1982. Excursions to Coniacian – Maastrichtian in the Austrian Alps. In: Working Group on Cretaceous Stage Boundaries, 4th Meeting, Vienna, 1982, pp. 1–104.

Kuhnt, W., Luderer, F., Nederbragt, S., Thurow, J., Wagner, T., 2005. Orbital-scale record of the late Cenomanian-Turonian oceanic anoxic event (OAE-2) in the Tarfaya Basin (Morocco). International Journal of Earth Sciences 94, 147–159.

Leckie, R.M., Bralower, T.J., Cashman, R., 2002. Oceanic anoxic events and plankton evolution: Biotic response to tectonic forcing during the mid-Cretaceous. Paleoceanography 17, 1041. doi:10.1029/2001PA000623.

Luciani, V., Cobianchi, M., 1999. The Bonarelli level and other black shales in the Cenomanian-Turonian of the northeastern Dolomites (Italy): calcareous nannofossil and foraminiferal data. Cretaceous Research 20, 135–167.

Manivit, H., Perch-Nielsen, K., Prins, B., Verbeek, J.W., 1977. Mid Cretaceous calcareous nannofossil biostratigraphy. Proceedings of the Koninklijke Nederlandse Akademie van Wetenschappen B80, 169–181.

Mattern, F., 2002. Amalgamation surfaces, bed thicknesses, and dish structures in sand-rich submarine fans: numeric differences in channelized and unchannelized deposits and their diagnostic value. Sedimentary Geology 150, 203–228.

Ogg, J.G., Agterberg, F.P., Gradstein, F.M., 2004. The Cretaceous period. In: Gradstein, F.M., Ogg, J.G., Smith, A.B. (Eds.), A Geological Time Scale 2004. Cambridge University Press, Cambridge, pp. 344–383.

Paul, C.R.C., Mitchell, S., Lamolda, M., Gorostidi, A., 1994. The Cenomanian-Turonian boundary event in northern Spain. Geological Magazine 131, 801–817.

Paul, C.R.C., Lamolda, M.A., Mitchell, S.F., Vaziri, M.R., Gorostidi, A., Marshall, J.D., 1999. The Cenomanian/Turonian boundary at Eastbourne (Sussex, UK): a proposed European reference section. Palaeogeography Palaeoclimatology Palaeoecology 150, 83–121.

Perch-Nielsen, K., 1985. Mesozoic calcareous nannofossils. In: Bolli, H.M., Saunders, J.B., Perch-Nielsen, K. (Eds.), Plankton Stratigraphy. Cambridge University Press, Cambridge, pp. 329–426.

Prey, S., 1952. Aufnahmen in der Flyschzone auf den Blättern Gmunden-Schafberg (4851) und Kirchdorf-Krems (4852) (Gschliefgraben), sowie auf den Blättern Ybbs (4754) und Gaming-Mariazell (4854) (Rogatsboden) (Bericht 1951). Verhandlungen der Geologischen Bundesanstalt 1952, 41–45.

Prey, S., 1983. Das Ultrahelvetikumsfenster des Gschliefgrabens südsüdöstlich von Gmunden (Oberösterreich). Jahrbuch der Geologischen Bundesanstait 126, 95–127.

Prokoph, A., Villeneuve, M., Agterberg, F.P., Rachold, V., 2001. Geochronology and calibration of global Milankovitch cyclicity at the Cenomanian-Turonian boundary. Geology 29, 523–526.

Sageman, B.B., Meyers, S.R., Arthur, M.A., 2006. Orbital time scale and new C-isotope record for Cenomanian-Turonian boundary stratotype. Geology 34, 125–128.

Schlanger, S.O., Arthur, M.A., Jenkyns, H.C., Scholle, P.A., 1987. The Cenomanian–Turonian oceanic anoxic event: I. Stratigraphy and distribution of organic-rich beds and the marine $\delta^{13}C$ excursion. In: Brooks, J., Fleet, A.J. (Eds.), Marine and Petroleum Source Rocks. Geological Society, London, Special Publication 26, 371–399.

Scopelliti, G., Bellanca, A., Coccioni, R., Luciani, V., Neri, R., Baudin, F., Chiari, M., Marcucci, M., 2004. High-resolution geochemical and biotic records of the Tethyan "Bonarelli Level" (OAE2, latest Cenomanian) from the Calabianca-Guidaloca composite section, northwestern Sicily, Italy. Palaeogeography Palaeoclimatology Palaeoecology 208, 293–317.

Snow, L.J., Duncan, R.A., Bralower, T.J., 2005. Trace element abundances in the Rock Canyon Anticline, Pueblo, Colorado, marine sedimentary section and their relationship to Caribbean plateau construction and oxygen anoxic event 2. Paleoceanography 20, PA3005. doi:10.1029/2004PA001093.

Stampfli, G.M., Borel, G., Marchant, R., Mosar, J., 2002. Western Alps geological constraints on western Tethyan reconstructions. Journal of the Virtual Explorer 8, 77–106.

Steuber, T., 2002. Plate tectonic control on the evolution of Cretaceous platform-carbonate production. Geology 30, 259–262.

Stover, L.E., 1966. Cretaceous coccoliths an associated nannofossils from France and the Netherlands. Micropaleontology 12, 133–167.

Strasser, A., Caron, M., Gjermeni, M., 2001. The Aptian, Albian and Cenomanian of Roter Sattel, Romandes Prealps, Switzerland: a high-resolution record of oceanographic changes. Cretaceous Research 22, 173–199.

Stradner, H., 1962. Über neue und wenig bekannte Nannofossilien aus Kreide und Alttertiär. Sonderdruck Verhandlungen der Geologischen Bundesanstalt 2, 363–377.

Swart, P.K., Burns, S.J., Leder, J.J., 1991. Fractionation of the stable isotope of oxygen and carbon in carbon dioxide during the reaction of calcite with phosphoric acid as a function of temperature and technique. Chemical Geology 86, 89–96.

Taylor, H., Teichmüller, M., Davis, A., Diessel, C.F.K., Littke, R., Robert, P., 1998. Organic Petrology. Borntraeger, Berlin-Stuttgart, 704 pp.

Tissot, B.T., Welte, D.H., 1984. Petroleum Formation and Occurrences, second ed. Springer Verlag, Berlin, 699 pp.

Tsikos, H., Jenkyns, H.C., Walsworth-Bell, B., Petrizzo, M.R., Forster, A., Kolonic, S., Erba, E., Premoli Silva, I., Baas, M., Wagner, T., Sinnighe Damsté, J.S., 2004. Carbon-isotope stratigraphy recorded by the Cenomanian-Turonian Oceanic Anoxic Event: correlation and implications based on three key localities. Journal of the Geological Society London 161, 711–719.

Varol, O., 1992. Taxonomic revision of the Polycyclolithaceae and its contribution to Cretaceous biostratigraphy. Newsletters on Stratigraphy 27, 93–127.

Voigt, S., 2000. Cenomanian-Turonian composite $\delta^{13}C$ curve for Western and Central Europe: the role of organic and inorganic carbon fluxes. Palaeogeography Palaeoclimatology Palaeoecology 160, 91–104.

Weidich, K.F., 1987. Das Ultrahelvetikum von Liebenstein (Allgäu) und seine Foraminiferenfauna. Zitteliana 15, 193–217.

Wendler, I., Wagreich, M., Neuhuber, S., Wendler, J., 2005. Development of highly oxic pelagic sedimentation in the lower Turonian – a high-resolution analysis (Buchberg, Austrian Alps). Geophysical Research Abstracts 7, 10805.